Proximity Effect in Fast Transient Simulations of an Underground Transmission Cable

Unnur Stella Gudmundsdottir

***Abstract*— This paper describes a method for including proximity effect calculations in EMT-based simulations. A subdivision of conductors FEM method is used to calculate conductor (core and sheath) impedances. A full phase impedance matrix is then constructed, including semiconductive layers, insulation layers and a special screen of two conducting materials. Finally the method is tested using the Universal Line Model and is verified against field measurements.**

***Keywords*: Insulated cables, modeling, power system transients, simulation, model accuracy, XLPE cables, wave propagation, modal excitation, proximity effect, EMT simulation**

Introduction

NOWADAYS, extruded (XLPE) cables are the most common cable types in high voltage (HV) underground cable systems. The XLPE cable type has the advantage of having no need for auxiliary equipment and no risk of leakage as the insulation is homogeneous and without any type of fluids. For studies of cable systems, such as insulation co-ordination, it is crucial to have accurate models.

EMT-based simulations for transient studies of cable lines use the Cable Constants (CC) method for calculating series impedance and shunt admittance of the cable [1]. Although very accurate for most studies, the equations in the CC method do not take an account for the proximity effect.

It has been discussed in [2] how lack of proximity effect can cause inaccurate simulations. It has furthermore been shown in [3] how, for the intersheath mode of propagation [4], there is inadequate damping of the signals for higher frequency oscillations (10 kHz and above). This is because of wrong imaginary part of the series impedance in the simulation which can be explained by the lack of including the proximity effect in the simulation software.

An analysis of a deviation between field measurements and simulation results has revealed how the wired part of the sheath conductor should be more accurately represented in the simulation software [3]. The analysis revealed how the wired characteristics of the metal screen of the HV cable and the proximity effect should be included in the series impedance calculations.

This paper describes the properties of an XLPE cable and addresses how the proximity effect can be modelled in detail in order to have more precise simulation results. Furthermore, in this paper, the improved modelling procedure is verified against field measurements and compared to CC method calculations.

U. S. Gudmundsdottir is a Senior Cable Specialist and Group Leader in the Transmission Department at Energinet.dk, 7000 Fredericia, Denmark (e-mail: usg@energinet.dk).

Paper submitted to the International Conference on Power Systems Transients (IPST2013) in Vancouver, Canada July 18-20, 2013.

I. Proximity Effect Variables

When AC currents flow in a conductor, the resulting magnetic flux will be time varying. When the frequency increases, the magnetic flux $\frac{d\emptyset}{dt}$ will vary more, resulting in larger eddy currents of adjacent conductors. Therefore, the higher the frequency, the stronger the proximity effect. An example of proximity effect is shown in Fig. 1.

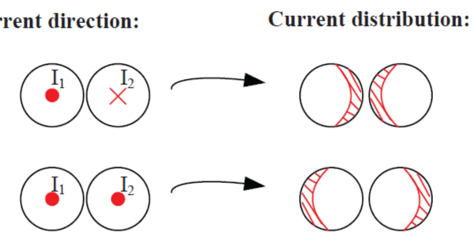

Fig. 1 Current distribution because of proximity effect for two adjacent conductors carrying current in the same direction and in opposite direction.

A HV single core XLPE cable often has a metal screen consisting of Cu wires and Al laminate, as shown in Fig. 2. The reason for this is radial water tightening. Without the Al laminate, there is a higher risk of the inner insulation becoming in contact with water.

Fig. 2 A typical layout for a HV XLPE cable

Due to the wire part of the screen, the proximity effect for wires with the same current direction causes the current distribution in the screens to be more non-homogen. This changes the series impedance of the cable at the higher frequencies and causes more damping. Furthermore, as the intersheath part of the cable current propagates between the screens of adjacent cables, their propagation characteristics are also affected by proximity effects between the three single core cables. It is therefore necessary to look more closely at each conducting layer in all cables, and divide them into a number of subconductors, for including the current distribution shown in Fig. 1.

II. Calculation Method

The cable model used is the frequency dependent phase model (FDPM), also called universal line model [4]. This model uses analytical CC method calculations of $Y(\omega)$ and $Z(\omega)$ for fitting the cables characteristic admittance Y_c and propagation function H in time domain [5].

For including the proximity effect, in this paper, the cables full phase impedance matrix of $Z(\omega)$ is externally calculated, by a FEM method programmed in MATLAB, and delivered as an output value to the FDPM. Therefore, in order to calculate the terminal conditions and simulate a cable line using FDPM, Z(ω) is used as an input to the EMT-based software and only Y (ω) is analytically calculated using the CC method. Based on this, the Universal Line Model then fits Y_c and H. The Universal Line Model is setup by The Manitoba HVDC Research Centre (owner and distributor of EMTDC/PSCAD). This has then been manipulated, such that it does not use analytical calculations, but imports Z(ω) from results obtained from FEM based calculations [6].

Dividing each conducting layer of the cable into a number of subconductors is a finite element (FEM) approach that assumes a constant current distribution and resistivity for each subconductor. By forming a conductor of a suitably large amount of subconductors, the non-uniformity in the current distribution because of skin and proximity effects is included. This method of subdividing the conductors has been used before [7], [8] and [9], where it is assumed that each intervening space (insulation in the cable) has the same and constant permeability. In this paper however, it is shown how to include different permeability for different intervening spaces, such as insulation and semiconductive (SC) layers for the case of a layered screen of wires, SC layer and an Al laminate. Furthermore, in this paper, the impedance of the earth return is included instead of using a fictitious return path.

A. Subdividing the conductors

The elemental subconductors proposed in [8] give a good image of the total impedances of the cable conductors, because of the non-uniformity of the current distribution. This is because of how the filaments are formed. They closely fill the entire volume of the real conductor and by distributing them exponentially there is even a larger amount of elements, where the current distribution is denser. Such a distribution indicates that the closer to the conductor surface, the larger amount and thinner the subconductors are, calculating more correctly for the non-uniformity of the current distribution. This distribution of filaments is shown in Fig. 3. Each element must be sized such that constant current density can be assumed. The non-uniform current distribution is obtained because of mutual coupling between elements and the fact that current density in one element can vary from the next.

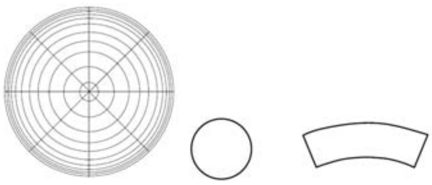

Fig. 3 Distribution of elements and element types for subdivision of conductors.

The elements are placed by use of x-y coordinates, where the (0,0) coordinate is the centre of one of the three AC cables. Cables in tight trefoil are placed as shown in Fig. 4. Similar can be used for cables in flat formation.

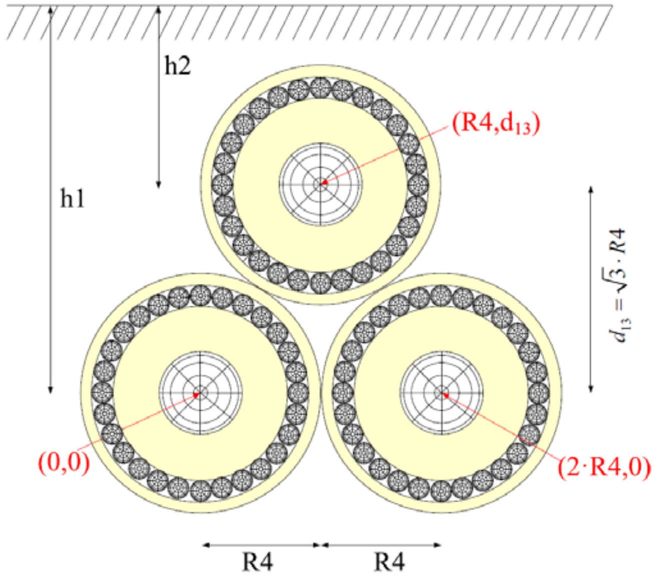

Fig. 4 Cross sectional layout for a three phase single core cable system with subdivision of conductors.

For calculating $Z(\omega)$, the self and mutual inductances of all elements and the geometric mean distance (GMD) for each element must be known. The GMD calculations are divided into self GMD, mutual GMD for elements far apart, and mutual GMD for close elements [6].

For the current in each element, a loop is formed through a fictitious lossless return path. Then it is possible to calculate the impedance of each element, where there is no total current flowing in the fictitious return.

A lumped equivalent scheme of the constant impedances for each element is shown in Fig. 5. The figure demonstrates three conductors of a single cable; core and two screens (Sh1 and Sh2). The screen is divided into two conductors, as it contains both a wire configuration and a laminate.

Each conductor of the cable is subdivided into n_1, n_2 and n_3 subconductors, and there are 3 cables. For the conductors of Fig. 5, the voltage/current relationship for a single cable is described by (1).

$$\begin{bmatrix} V_C \\ V_{Sh1} \\ V_{Sh2} \end{bmatrix} = [R]\cdot\begin{bmatrix} I_C \\ I_{Sh1} \\ I_{Sh2} \end{bmatrix} + j\omega[L]\begin{bmatrix} I_C \\ I_{Sh1} \\ I_{Sh2} \end{bmatrix} \quad (1)$$

Where [R] and [L] are resistance and inductance matrices of size NxN witn $N=n_1+n_2+n_3$, C denotes the cable conductor, *Sh1* denotes the wired part of the screen and *Sh2* denotes the Al laminate part of the screen.

For an element with uniform current distribution, the resistance is calculated from (2), for each element i of a conductor n.

$$R_i = \frac{\rho_n}{A_i} \quad (2)$$

Where ρ is the constant resistivity of conductor n, A is the surface area of subconductor I and each element has constant current distribution and resistivity.

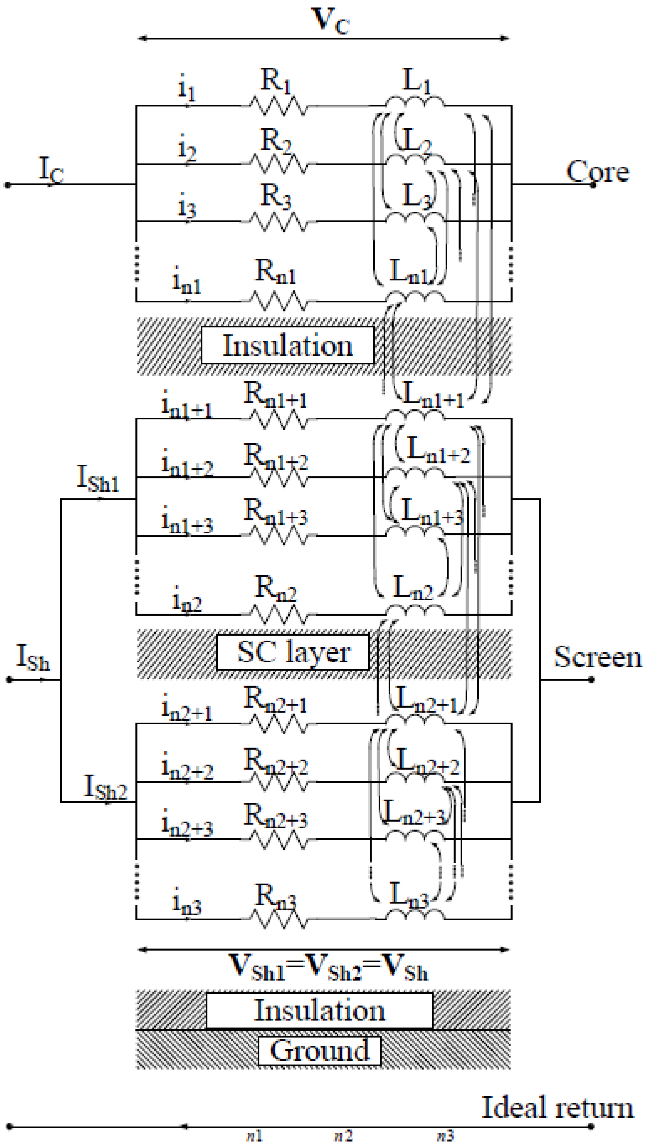

$$I_{return} = \sum_{k=1}^{n1} i_k + \sum_{k=n1+1}^{n2} i_k + \sum_{k=n2+1}^{n3} i_k$$

Fig. 5 Equivalent impedance scheme of the lumped constant parameters for subdivision of conductors of one cable. The dots illustrate a continuing (as previous) further many connections.

The inductance is divided into loop self-inductance and mutual inductance between two loops, where the loop is through a fictitious lossless return path.

The mutual inductance is caused by current flowing in one loop due to flux linkage with a loop containing current. This is described by (3) for linear medium, such as each subconductor with uniform resistivity and current distribution.

$$L_{ii} = \frac{\Psi_{ii}}{I_i} \qquad L_{ij} = \frac{\Psi_{ij}}{I_i} \tag{3}$$

Where L_{ii} is the flux linkage in the loop itself, per unit current and L_{ij} is the flux linkage from loop j to loop i, per unit current.

In order to calculate the flux linkage, the magnetic field due to an element itself, and between two elements, with the fictitious return path, must be calculated (4).

$$\Psi = \int_{D_{ij}}^{D_{iq}} \frac{\mu_o \mu_i I_i}{2\pi} \frac{1}{x} dx + \int_{D_{q1q2}}^{D_{jq}} \frac{\mu_0 \mu_q I_i}{2\pi} \frac{1}{x} dx = \frac{\mu_0 I_i \mu}{2\pi} \ln\left(\frac{D_{iq} D_{jq}}{D_{ij} D_{q1q2}} \right) \tag{4}$$

Where the first part is for element i to element j with fictitious return, and the second part is for return to itself and back to element j. D is the GMD between two current paths, q is the fictitious return path and μ is the permeability.

Based on (3) and (4), the self and mutual inductances for the elements can be calculated using (5), where *ln(D)* is a logarithmic mean distance.

$$L_{ii} = \frac{\Psi_{ii}}{I_i} = \frac{\mu_0 \mu}{2\pi} \ln\left(\frac{r_q}{D_{ii}}\right) \qquad L_{ij} = \frac{\Psi_{ij}}{I_i} = \frac{\mu_0 \mu}{2\pi} \ln\left(\frac{r_q}{D_{ij}}\right) \tag{5}$$

Where the current path chosen is circular with radius r_q, much larger than the GMD_{iq} for any element i, and hence $D_{iq}=D_{jq}=D_{q1q2}=r_q$ [9].

B. Impedance matrix for conducting layers

Based on (1), (2) and (5), the impedance matrix including three conductors for each cable, divided into subconductors, can be calculated as shown in (6).

$$\begin{bmatrix} [R_{C1}] & & \\ & [R_{C2}] & \\ & & [R_{C3}] \end{bmatrix} + j\omega \begin{bmatrix} [L_{C1}] & [L_{C1C2}] & [L_{C1C3}] \\ [L_{C1C2}] & [L_{C2}] & [L_{C1C2}] \\ [L_{C1C3}] & [L_{C2C2}] & [L_{C3}] \end{bmatrix} \tag{6}$$

Where c1, c2 and c3 denote cables 1, 2 and 3 respectively. *[Rck]* and *[Lck], k=1,2 and 3,* are each of the size *NxN*, with $N= n_1+n_2+n_3$.

The desired impedance matrix, for three single core cables, is a 6x6 matrix, for every frequency point. In order to obtain such a 6x6 matrix, first the two screen layers must be joined into one, and then the remaining matrix must be reduced to form only a single element for all 6 conductors (3 cores and 3 screen conductors). The matrix of (6) is reduced using bundling of conductors.

Bundling of conductors is a procedure used for Overhead Lines in [10], but has in this paper been adapted for cable systems. When several impedances are connected in parallel, it is possible to eliminate all except one voltage/current relationships, and hence reduce the impedance matrix. This is due to the fact that the voltages across each impedance are equal, because of the parallel connection. It is therefore possible to bundle the two screen layers, even though they are made of entirely different materials and separated by a SC layer. After reducing the two layers of the screen into a single conductor, divided into n_2 subconductors, the size of the impedance matrix has been reduced from NxN to $N'xN'$, where $N'=n_1+n_2$ for each cable.

A similar reduction method is used again in order to remove all subconductor rows/columns, except for the first row/column of every main conductor (i.e. 3 cores and 3 screens). Finally the impedance matrix will be as in (7).

$$Z_{reduced} = \begin{bmatrix} Z_{C1cc} & 0 & 0 & Z_{C1cs} & 0 & 0 \\ 0 & Z_{C2cc} & 0 & 0 & Z_{C2cs} & 0 \\ 0 & 0 & Z_{C3cc} & 0 & 0 & Z_{C3cs} \\ Z_{C1cs} & 0 & 0 & Z_{C1ss} & Z_{C1ssC2ss} & Z_{C1ssC3ss} \\ 0 & Z_{C2cs} & 0 & Z_{C1ssC2ss} & Z_{C2ss} & Z_{C2ssC3ss} \\ 0 & 0 & Z_{C3cs} & Z_{C1ssC3ss} & Z_{C2ssC3ss} & Z_{C3ss} \end{bmatrix} \quad (7)$$

Where Z_{Ckcc} is the impedance of the core conductor for cable k, Z_{Ckcs} is the impedance of the mutual between core and screen of cable k, Z_{Ckss} is the impedance of the screen conductor for cable k, $Z_{CkssCrss}$ is the impedance between screens of cables k and r. There is no mutual impedance between cores of two cables because they are screened, and there is no mutual impedance between core-screen loops of two cables.

In the above calculations a fictitious lossless return path has been used. For calculating the loop impedance between the core and screen, using impedance of the earth return instead, screen voltage shall be subtracted from the core voltage (8). This can be done, there is no total current flowing in the fictitious return. When there is no total current flowing in the fictitious return, then for each cable $[I_{Sh}] = -[I_C]$.

$$\begin{bmatrix} V_C - V_{Sh} \\ V_{Sh} \end{bmatrix} = \begin{bmatrix} Z_{CC} - Z_{CS} & Z_{CS} - Z_{SS} \\ Z_{CS} & Z_{SS} \end{bmatrix} \cdot \begin{bmatrix} I_C \\ -I_C \end{bmatrix} \quad (8)$$

After the subtraction, (7) is replaced with (9), where the fictitious lossless return path is removed.

$$Z_{reduced} = \begin{bmatrix} Z_{C1cc} & 0 & 0 & Z'_{C1cs} & 0 & 0 \\ 0 & Z_{C2cc} & 0 & 0 & Z'_{C2cs} & 0 \\ 0 & 0 & Z_{C3cc} & 0 & 0 & Z'_{C3cs} \\ Z_{C1cs} & 0 & 0 & Z_{C1ss} & Z_{C1ssC2ss} & Z_{C1ssC3ss} \\ 0 & Z_{C2cs} & 0 & Z_{C1ssC2ss} & Z_{C2ss} & Z_{C2ssC3ss} \\ 0 & 0 & Z_{C3cs} & Z_{C1ssC3ss} & Z_{C2ssC3ss} & Z_{C3ss} \end{bmatrix} \quad (9)$$

Where $Z'_{Ckcs} = Z_{Ckcc} - 2Z_{Ckcs} + Z_{Ckss}$.

(9) is the impedance matrix of only the conducting layers. Section C will include the impedance of all other layers and ground return.

C. Full impedance matrix

The proximity effect only appears in conducting material, as it is related to current distribution because of magnetic field of two close conductors. Therefore only conductors are subdivided. For obtaining the full impedance matrix for cable simulations, the impedances of insulation layers and ground must be included. The impedance of the non-conducting layers can be calculated by (10).

$$Z_{inner-insul}(\omega) = \frac{j\omega\mu_{inner-insul}}{2\pi} \ln\left(\frac{r_2}{r_1}\right) \quad (10)$$

$$Z_{outer-insul}(\omega) = \frac{j\omega\mu_{outer-insul}}{2\pi} \ln\left(\frac{r_4}{r_3}\right)$$

Where $\mu_{inner-insul}$ and $\mu_{outer-insul}$ are the inner and outer insulation permeability, r_2 and r_1 are the outer and inner radius of the inner insulation and r_4 and r_3 are the outer and inner radius of the outer insulation.

It is shown in [6], how at higher frequencies the ground return has negligible influence on the simulation results. Furthermore, the proximity effect only has influence at higher frequencies. Therefore, for studies requiring the subdivision of conductors, most often analytical calculations for the ground impedance will be sufficient, and the ground impedance can be calculated as normally done in the CC method, by [11], [12], [13], [14].

For cases, when ground return needs to be more accurately simulated, it is possible to add the ground as another conductor to be subdivided by the same principles as previously explained. The size of the ground subconductors should be made smaller close to the cables, than farther away. This can be obtained by an exponential distribution of subconductors.

Finally the full impedance matrix of a three phase AC cable system, with subdivision of conductors can be calculated by (11). Here the different insulation layers, having unique permeability, and ground return is included.

$$Z_{full} = \begin{bmatrix} Z_1^1 & -Z_{SM}^1 & Z_{gm12} & Z_{gm12} & Z_{gm13} & Z_{gm13} \\ -Z_{SM}^1 & Z_2^1 & Z_{gm12} & Z_{gm12} & Z_{gm13} & Z_{gm13} \\ Z_{gm12} & Z_{gm12} & Z_1^2 & -Z_{SM}^2 & Z_{gm23} & Z_{gm23} \\ Z_{gm12} & Z_{gm12} & -Z_{SM}^2 & Z_2^2 & Z_{gm23} & Z_{gm23} \\ Z_{gm13} & Z_{gm13} & Z_{gm23} & Z_{gm23} & Z_1^3 & -Z_{SM}^3 \\ Z_{gm13} & Z_{gm13} & Z_{gm23} & Z_{gm23} & -Z_{SM}^3 & Z_2^3 \end{bmatrix} \quad (11)$$

Where each impedance of the matrix is given by (12), for cables k and r.

$$\begin{aligned} Z_1^k &= Z_{Ckcc} + Z_{Ck\,inner-insul} + Z_{Ck\,outer-insul} + Z_{Ck\,ground} \\ Z_2^k &= Z_{Ckss} + Z_{Ci\,outer-insul} + Z_{Ck\,ground} \\ Z_{SM}^k &= Z'_{Ckcs} + Z_{Ck\,outer-insul} + Z_{Ck\,ground} \\ Z_{gmkr}^k &= Z_{Ckss\,Crss} + Z_{Ckr\,ground} \end{aligned} \quad (12)$$

III. Comparison of Field Measurements and Simulations

The new modeling procedure of including proximity effect is tested against field measurements. Furthermore, it is compared to simulations using the classical CC-method.

A. Field measurements

In order to verify the new modeling procedure, the intersheath mode is excited. In other words, the current loop is formed by the sheath of one cable with the sheath of an adjacent cable as return. The reason for this is because when the intersheath mode is excited, the proximity effect of the wires in the screen will affect the results as there is current propagation between the screens of two adjacent cables.

The cable line used in this paper consists of a three phase cable system with 150 kV single core 1200 mm^2 XLPE cables. The cables are laid in a tight trefoil with the bottom cables at 1.3 m depth, and the measurement setup is shown in Fig. 6.

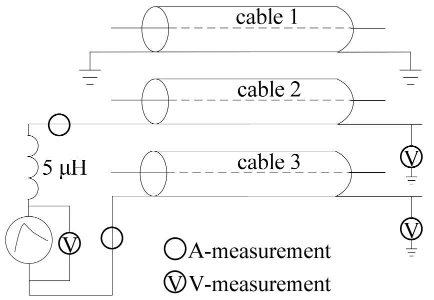

Fig. 6 Measurement setup for excitation of an intersheath mode.

In the measurement setup, a fast front impulse is used to energise between two sheaths (cable 2 and 3), while the third sheath is grounded. All core conductors are kept open at both sending and receiving end. Sheath voltages at both sending and receiving end of cables 2 and 3 and sheath currents of cables 2 and 3 at sending end were measured. The generator used is a HAEFELY PC6-288.1 surge tester. It is used to generate a 2 kV 1.2/50 µs impulse shown in Fig. 7.

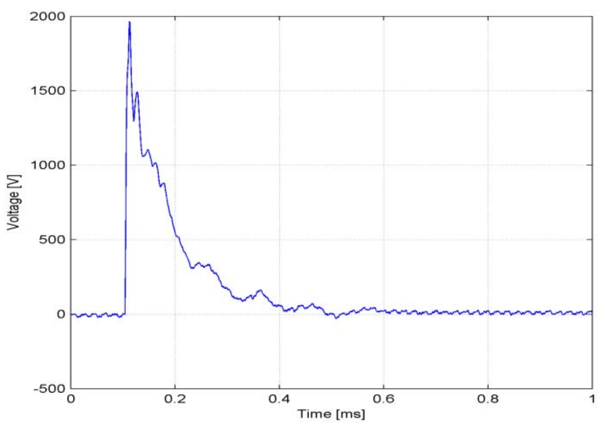

Fig. 7 Impulse voltage for excitation of the intersheath mode. This is the measured core voltage at the sending end of the excited sheath.

Identical Tektronix TDS 3014B oscilloscopes were used for measuring at both cable ends and the data was logged into a computer. For all tests, Tektronix HV probes are used and for current measurements a PEM RGF15 was used to measure the sheath currents at the sending end.

B. Simulations

The cable parameters, used for modeling purposes, are given in Table I and a cross section of the cable is shown in Fig. 8. The parameters are already corrected according to the theory [6], [15].

The simulations for the classical CC method are performed using the frequency dependent phase model in EMTDC/PSCAD where the measured excitation voltage in Fig. 7 is used as an input to the simulation model. This ensures that the excitation sending end voltage is identical for simulations and field tests.

For including the proximity effect, the $Z(\omega)$ calculations are performed in MATLAB, for the same cable parameters. The cables are laid in a tight trefoil at depth 1.3 m. The impedance matrix (11) is calculated and used as an input to the FDPM model given by The Manitoba HVDC Research Centre.

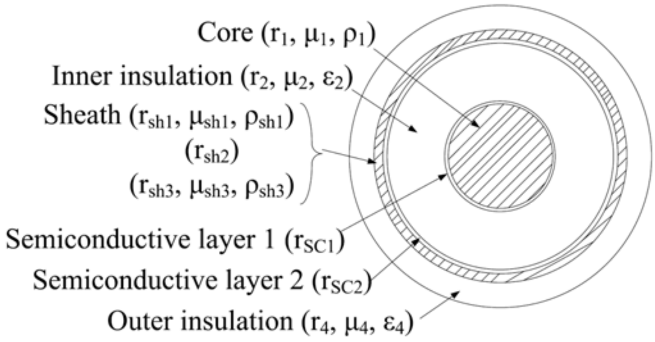

Fig. 8 Cross section of one single core cable showing the cable characteristic.

TABLE I
CABLE PARAMETERS

Parameter	Value
Stranded conductor, 1200mm^2 AL	r_1=20.75 mm, $\rho_1=3.19\cdot10^{-8}$ Ωm, μ_1=1.0
Semiconductive layer 1	r_{SC1}=22.25 mm
Inner insulation	r_2=39.25 mm, ε_2=2.68, μ_2=1.05
Semiconductive layer 2	r_{SC2}=40.25 mm
Stranded sheath, 95mm^2 Cu	r_{sh1}=41.96 mm $\rho_{sh1}=0.91\cdot10^{-7}$ Ωm, μ_{sh1}=1.0
Sheath SC	r_{sh2}=42.56 mm
Laminate sheath, Al	r_{sh3}=42.76 mm $\rho_{sh3}=2.83\cdot10^{-8}$ Ωm, μ_{sh3}=1.0
Outer insulation	r_4=47.94 mm, ε_4=2.3, μ_4=1.0
Cable length	l=1.78 km
Earth return	ρ_{earth}=100 Ωm

For the validation and comparison, the sending end current, and the receiving end voltage are compared for simulations with, and without proximity affect, as well as for field measurements. These results are shown in Fig. 9 - Fig. 10.

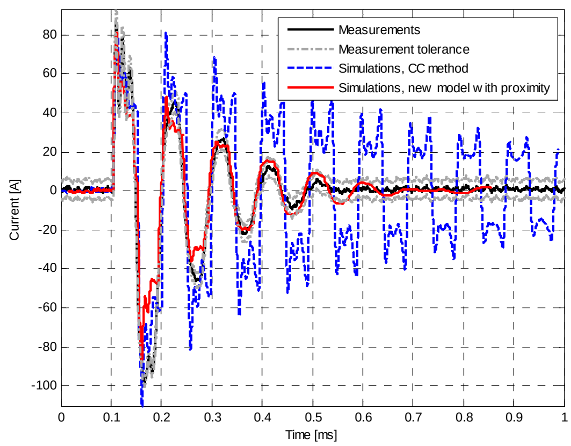

Fig. 9 Comparison of the sending end current on energized scree, cable 2 in Fig. 6, for the intersheath mode. The figure compares field measurements with simulations using the traditional CC method and with simulations including proximity effect

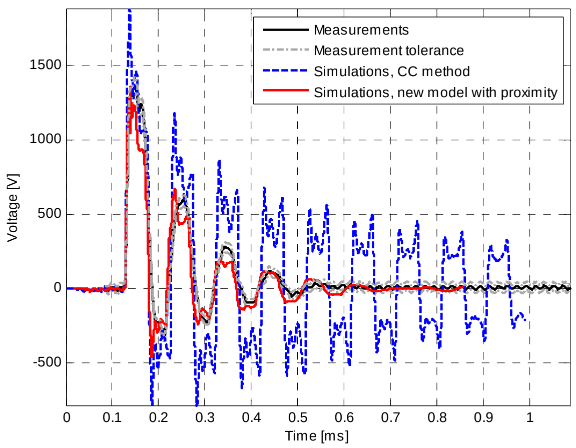

Fig. 10 Comparison of the receiving end voltage on energized scree, cable 2 in Fig. 6, for the intersheath mode. The figure compares field measurements with simulations using the traditional CC method and with simulations including proximity effect

As shown in Fig. 9 - Fig. 10, the simulation results are very accurate when the proximity effect, with correct physical layout of the screen, is included. There is almost a perfect agreement between improved simulations and field measurement results.

Another conclusion drawn from the results in Fig. 9 - Fig. 10, is regarding the simulation time. The calculations of *Z(ω)* by use of subdivision method requires larger amount of calculations and simulation time, compared to the analytical calculations of CC method. The subdivision calculations on the other hand, only need to be performed once, for each cable, as they will not change when terminal connections of the cable are changed. For simulations having wrong high frequency oscillations, as shown for the analytical calculations in Fig. 9 - Fig. 10, in order to ensure convergence of the simulations using the CC method, the simulation time step for every simulation shall be very small. This requires long simulation time for each and every study performed using an EMT-program with CC method only. On the other hand, for the method including proximity effect, when the impedance has been correctly calculated once, the simulation time step for every simulation study of the cable system, can be increased. This is because the high frequency oscillations have been removed. This will in turn lower the simulation time for every cable system study performed, as the risk of non-convergence is much smaller, and total simulation time for studies with proximity effect becomes less than without including proximity effect.

IV. Conclusions

In this paper, improvements for fast transient cable modelling by including proximity effect in EMT-based simulation software is discussed. A FEM method called subdivision of conductors is used to include proximity effect in high frequency impedance calculation, used for fast transient simulations. A full phase frequency dependent impedance matrix is constructed, to be used in EMT-based software instead of normally used CC Calculations. The simulation method is finally validated against field measurements on a 150 kV underground cable.

The simulation results including the proximity effect show large improvements when compared to field measurements, where high frequency oscillations due to lack of damping are removed. The results show, how transient studies for normal XLPE cables with wires in the cable screen can highly benefit from using the proposed FEM method both regarding accuracy and overall system study time. Therefore, from this improved modelling method, proximity effect can be included in EMT-based simulations, making damping in fast transient simulations correct, compared to field measurements.

References

[1] A. Ametani, "A general formulation of impedance and admittance of cables," *IEEE Transactions on Power Apparatus and Systems*, vol PAS-99, no. 3, pp.902-910, May/June 1980.

[2] B. Gustavsen, J. Sletbak, and T. Henriksen, "Simulation of transient sheath overvoltages in the presence of proximity effects", *IEEE Trans. Power Delivery*, vol. 10, no. 2, pp. 1066-1075, April 1995

[3] U. S. Gudmundsdottir, J. De Silva, C. L. Bak and W. Wiechowski, "Double Layered Sheath in Accurate HV XLPE Cable Modeling", *IEEE PES GM 2010 in Minneapolis, USA*, July 2010.

[4] B. Gustavsen, *A study of overvoltages in high voltage cables with emphasis on sheath overvoltages*. Trondheim, Norway: PhD. Thesis, NTH, 1986.

[5] B. Gustavsen, A. Morched and M. Tartibi, "A universal model for accurate calculation of electromagnetic transients on overhead lines and underground cables," *IEEE Trans. On Power Delivery*, vol. 14, no. 3, pp. 1032-1038, july 1999.

[6] U. S. Gudmundsdottir, *Modelling of long High Voltage AC cables in Transmission Systems*. Fredericia: Energinet.dk, Aalborg Univercity, 2010, ISBN: 978-87-90707-73-6.

[7] P. de Arizon and H. W. Dommel, "Computation of cable impedances based on subdivision of conductors." *IEEE Transactions on Power Delivery*, vol. PWRD-2, no. 1, pp. 21-27, January 1987.

[8] R. Lucas and S. Talukdar, "Advances in finite element techniques for calculating cable resistances and inductances," *IEEE Transactions on Power Apparatus and Systems*, vol. PAS-97, no. 3, pp. 875-883, May/June 1978.

[9] R. A. Rivas and J. R. Martí, "Calculation of frequency-dependent parameters of power cables: matrix partitioning techniques," *IEEE Transactions on Power Delivery*, vol. 17, no. 4, pp. 1085-1092, October 2002.

[10] M. H. Hesse, "Electromagnetic and alectrostatic transmission-line parameters by digital computer," *IEEE Transactions on Power Apparatus and Systems*, vol. 82, no. 66, pp. 282-291, June 1963.

[11] V. F. Pollaczek, "Über das feld einer unendlich langen wechselstromdurchflossenen einfachleitung (in german)," *Elektrische Nachrichtentechnik*, vol. 9, no. 3, pp. 339-360, July 1926.

[12] L. Wedepohl and D. Wilcox, "Transient analysis of underground power-transmission systems," *IEE Proceedings*, vol. 120, no. 2, pp. 253-260, February 1973.

[13] O. Saad, G. Gaba, and M. Giroux, "A closed-form approximation for ground return impedance of underground cables," *IEEE Transactions on Power Delivery*, vol. 11, no. 3, pp. 1536-1545, July 1996.

[14] H. W. Dommel, EMTP Theory Book, 2nd ed. Vancouver, British Columbia Canada: Microtran Power System Analysis Corporation, Vancouver, British Columbia, 1996.

[15] J.A. Martinez, B. Gustavsen and D. Durbak, "Parameter determination for modelling system transients - part II: insulated cables," *IEEE Transactions of Power Delivery*, vol. 20, no. 3, pp. 1045-2050, July 2005.